



Enhancement of antiproliferative activity by molecular simplification of catalpol

Celina García^{a,*}, Leticia G. León^{a,b}, Carlos R. Pungitore^c, Carla Ríos-Luci^a, Antonio H. Daranas^{a,d}, Juan C. Montero^e, Atanasio Pandiella^e, Carlos E. Tonn^c, Víctor S. Martín^{a,*}, José M. Padrón^{a,b,*}

^a Instituto Universitario de Bio-Organica 'Antonio González' (IUBO-AG), Universidad de La Laguna, C/Astrofísico Francisco Sánchez 2, 38206 La Laguna, Spain

^b BioLab, Instituto Canario de Investigación del Cáncer (ICIC), C/Astrofísico Francisco Sánchez 2, 38206 La Laguna, Spain

^c INTEQUI-CONICET, Facultad de Química, Bioquímica y Farmacia, Universidad Nacional de San Luis, Chacabuco y Pedernera-5700-San Luis, Argentina

^d Departamento de Ingeniería Química y Tecnología Farmacéutica, Universidad de La Laguna, Avda. Astrofísico Francisco Sánchez s/n, 38206 La Laguna, Spain

^e Centro de Investigación del Cáncer, IBMCC/CSIC-Universidad de Salamanca, Campus Miguel de Unamuno. 37007 Salamanca, Spain

ARTICLE INFO

Article history:

Received 9 September 2009

Revised 19 February 2010

Accepted 22 February 2010

Available online 1 March 2010

Keywords:

Antitumor agents

Catalpol

Cell cycle

Molecular simplification

Structure elucidation

ABSTRACT

Two iridoid scaffolds were synthesized enantioselectively using as key step an L-proline-catalyzed α -formyl oxidation. The in vitro antiproliferative activities were evaluated against a representative panel of human solid tumor cell lines. Both iridoids induced considerably growth inhibition in the range 0.38–1.86 μ M. Cell cycle studies for these compounds showed the induction of cell cycle arrest at the G₁ phase. This result was consistent with a decrease in the expression of cyclin D1. Damaged cells underwent apoptosis as indicated by specific Annexin V staining.

© 2010 Elsevier Ltd. All rights reserved.

1. Introduction

Molecular simplification represents a drug design strategy to shorten synthetic routes while keeping or enhancing the biological activity of any given natural or synthetic template. Initially, this concept was applied empirically to natural products with complex structures in order to obtain active derivatives with a simplified molecular structure. Classical examples of molecular simplification are the natural alkaloids morphine and quinine, which led to several drugs currently used in therapy. The molecular simplification approach is particularly interesting in the development of new antitumor drugs, since a large number of current anticancer chemotherapeutics is derived from natural products that have complex chemical structures.¹ Recently, a series of simplified ecteinascidin² and epothilone³ analogs have been synthesized and evaluated, showing promising results. In this particular context, we have reported novel antiproliferative acetogenin analogs synthesized in a limited number of chemical steps.⁴

Within our research program directed toward the discovery of novel antiproliferative molecules, we have shown that naturally

occurring sugiol (**1**)⁵ and catalpol (**2**)⁶ can be transformed into antiproliferative drugs in a straightforward manner. Catalpol (**2**) shows significant in vitro inhibition of *Taq* DNA polymerase.⁷ Structurally this metabolite illustrates a certain resemblance with a nucleoside framework (Fig. 1). The bicyclic aglycone is alike the purine scaffold present in nucleosides and that could explain the observed *Taq* DNA polymerase inhibitory activity.^{4,7b} DNA polymerase inhibitors represent important drugs in anticancer or antiviral therapy, such as the deoxycytidine analogs ara-C (1- β -D-

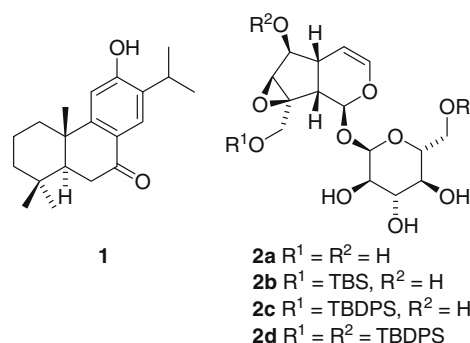


Figure 1. Structure of naturally occurring sugiol (**1**) and catalpol (**2**).

* Corresponding authors. Tel.: +34 922316502x6126; fax: +34 922318571.

E-mail addresses: cgargon@ull.es (C. García), vmartin@ull.es (V.S. Martín), jmpadron@ull.es (J.M. Padrón).

arabinofuranosyl-cytosine) and gemcitabine (2',2'-difluorodeoxycytidine, dFdC).⁸ These drugs belong to the group of antimetabolites. Examples of molecular simplified antimetabolites (lacking the sugar moiety) are the purine analogs 6-mercaptopurine and thioguanine, and the pyrimidine analog 5-fluorouracil.

Herein we report on the synthesis and biological evaluation of a simplified analog of the bicyclic aglycone of catalpol (**2**).

2. Results and discussion

2.1. Chemistry

Inspired by the chemical architecture of this iridoid, we envisioned the bicyclic core construction similar to that using by Mangion and MacMillan in the total synthesis of brasoside and littoralisone.⁹ The synthesis of the compounds reported in this study began from β -citronellol (**3**) and is outlined in Scheme 1. Thus, benzylation of the primary alcohol group led to ester **4**, which was converted into aldehyde **5** by ozonolysis. Applying the proline-catalyzed α -formyl oxidation protocol using L-proline over aldehyde **5**,¹⁰ followed by olefination of the resultant aldehyde using Horner–Wadsworth–Emmons conditions, produced (*E*)- α,β -unsaturated ester **6**. The secondary hydroxyl group was protected as its *tert*-butyldiphenylsilyl (TBDPS) ether and the resulting structure **7** was subsequently treated with DIBAL–H providing us the diol **8**. Dess–Martin oxidation of compound **8**, exposure of the dialdehyde intermediate to L-proline in DMSO, and subsequently acetylation provided the bicyclic derivative **9**.

2.2. Relative configuration

The relative configuration of the chiral centers in **9a** was determined mainly by the observed dipolar correlations in the NOESY spectrum, since the *J*-based configurational analysis was inconclusive. Considering that the relative configuration of the chiral centers in C-5 and C-7 is clear as resulted from the aforementioned asymmetric synthesis¹⁰ and from the starting material respectively, we will refer our results to them. Therefore, H-5 (δ_{H} 4.25) showed strong NOE cross-correlation peaks with H-4a (δ_{H} 2.5), H-7a (δ_{H} 1.6) and the methyl group at C-7 position (δ_{H} 0.85), indicating that all of them are in the same side of the bicyclic system. In the same way, H-4a (δ_{H} 2.5) showed a strong connectivity with H-7a (δ_{H} 1.6), confirming that the existence of a cis-type ring closure. These data allowed us to determine relative stereochemistries at C-4a, C-7a, C-5, and C-7 as 4a*S*,5*R*,7*R*,7a*S*. Likewise, the relative configuration of C-1 was determined mainly by analysis of the NOESY experiment. This time, NOE cross-correlations were

observed between H-1 and H-7a, H-7, methyl group at C-7 position and a weak and intriguing one with the methyl groups of the *tert*-butyl moiety. However, with the exception of the last one, these NOEs could be possible for both C-1 epimers.

A solution for this problem is suggested based on the results of a molecular mechanics approach to determine the relative configuration of these chiral centers in combination with NMR data.

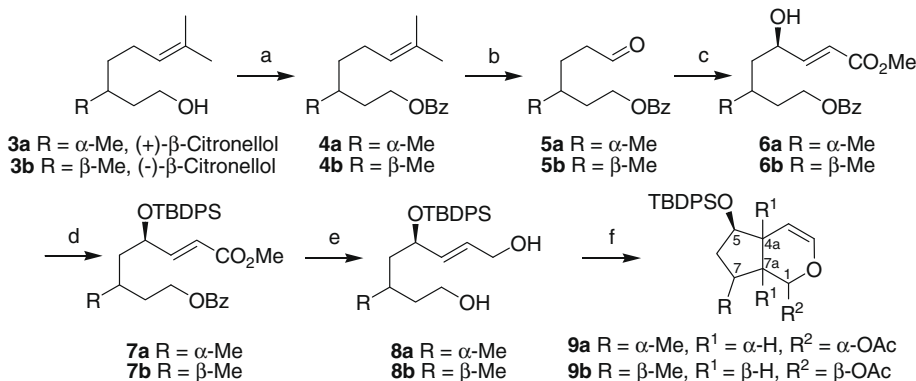
Once the planar structure and the stereochemistry of most chiral centers of **9a** were determined, a conformational study was carried out in order to determine the configuration of carbon C-1. Therefore, we decided to study the two possible isomers 1*R** and 1*S**. For that reason, Monte Carlo Multiple Minimum (MCM) conformational searches were undertaken.

These consisted of two independent searches with the MM2*¹¹ force field as implemented in MacroModel 8.5¹² using the generalized Born/surface area (GBSA) chloroform solvent model.¹³ Random searches of 5000 MCM steps were undertaken for each diastereoisomer to insure that the potential energy surface was thoroughly explored using the TNC algorithm. All local minima within 50 kJ of the global minimum were saved. The global minimum was found 97 times for each search, indicating that a thorough search of the molecule's potential energy surface was done.¹²

For the 1*R** (**9a**) isomer, the conformational search resulted in two conformational families with some differences into the bicyclic ring (Fig. 2). The orientation of H-1 in these molecules changes from being located in axial position in the best energy structure to an equatorial position in the best energy representative of the other conformational family ($\Delta E = +3.5$ kJ/mol). In the same way, for the 1*S** epimer, the results obtained were quite similar. Again two conformational families where the orientation of H-1 changes from equatorial in the best energy solution to an axial position in the other family ($\Delta E = +3.5$ kJ/mol) were found.

However, some important clues to find the solution of our problem were found. The conformational search conducted for the 1*S** epimer resulted in conformations where either H-1 and H-4a (2.8 Å) or the methyl groups of the acetate and the *tert*-butyl groups (3.3 Å) should be close enough to expect a clear but unobserved NOE correlations. On the other hand, the results obtained for the 1*R** epimer did not show such inconsistencies and at the same time could explain the intriguing NOE between H-1 and the methyls of the *tert*-butyl group, as one set of structures showed appropriated distances (2.35 Å).

The results of these simulations fully agree with experimentally measured $^3J_{\text{H-H}}$. In fact, it should be noted that the resulting ensemble-averaged (derived from the estimated populations by a Boltzmann distribution at 300 K) structures obtained from the MCM searches and the experimentally measured values matched



Scheme 1. Reagents and conditions: (a) BzCl, Et₃N, CH₂Cl₂, 99%; (b) (i) O₃, Py, CH₂Cl₂/MeOH (9:1), -78 °C; (ii) PPh₃, -78 °C to 0 °C, 91%; (c) (i) L-proline, PhNO, DMSO; (ii) (MeO)₂P(O)CH₂CO₂Me, DBU, LiCl, CH₃CN, -15 °C; (iii) NH₄Cl, MeOH, -15 °C to rt, 24%; (d) TBDPSCl, imidazole, CH₂Cl₂, rt, 94%; (e) DIBAL-H, Et₂O, -78 °C, 45%; (f) (i) DMP, CH₂Cl₂, rt; (ii) L-proline, DMSO, 40 °C, 60 h; (iii) Ac₂O, DMAP, Py, 0 °C, 15%.

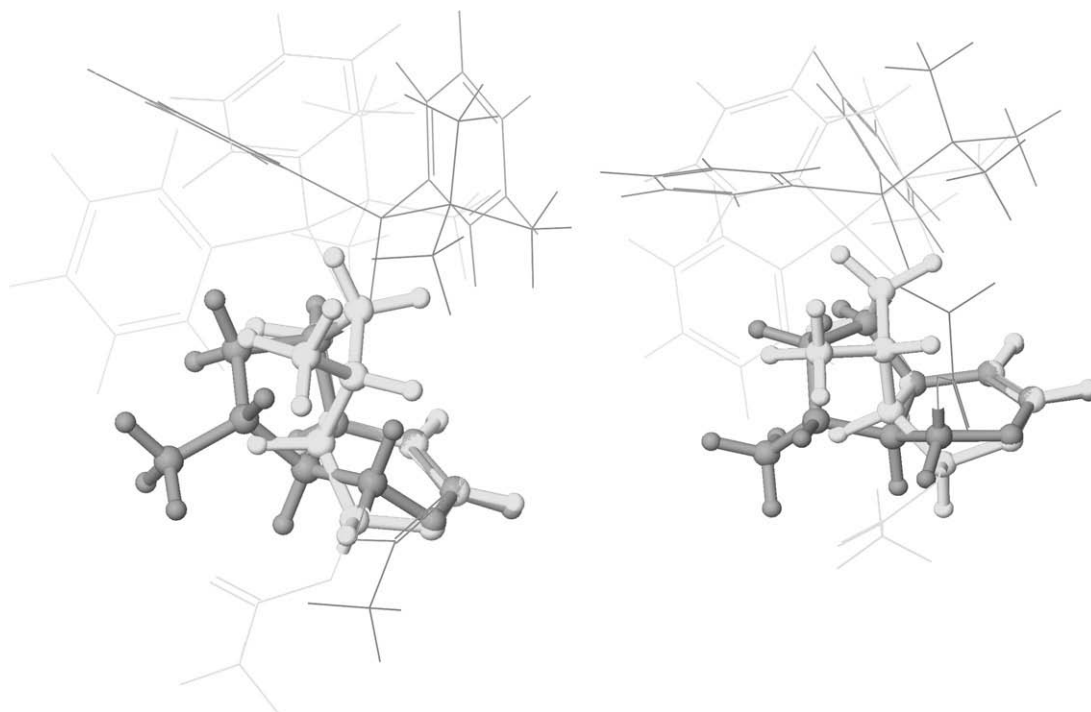


Figure 2. Comparison of the two different structural motifs found out of the MCMM conformational search conducted for the 1R* and 1S* epimers of **9a**. In clear gray the best energy conformer and in dark gray the best energy representative of the second conformational motif for the 1R* (left) and 1S* (right) epimers of **9a**.

very well. Even though **9a** is a rigid molecule, it shows some flexibility along the five and six membered-rings. Next, the results obtained from the simulations were compared to the NMR data available for **9a** and the outcome of such comparisons was that the energy-averaged structure matched appropriately with the experimental NMR data. In this way, the calculated values for those couplings using the Díez–Altona–Donders equations, as implemented in the software MSpin,¹⁴ were $^3J_{\text{H4a-H7a}} = 6.2$ Hz, $^3J_{\text{H7a-H1}} = 3.4$ Hz, $^3J_{\text{H7a-H7}} = 8.1$ Hz, and $^3J_{\text{H4a-H5}} = 5.1$ Hz, in excellent agreement with the corresponding experimentally measured values ($^3J_{\text{H4a-H7a}} = 6.3$ Hz, $^3J_{\text{H7a-H1}} = 2.7$ Hz, $^3J_{\text{H7a-H7}} = 7.5$ Hz, and $^3J_{\text{H4a-H5}} = 4.2$ Hz).

Consequently, based on the previous analysis (NOESY, $^3J_{\text{H-H}}$ couplings and MCMM simulations) we propose the 1R,4aS,5R,7-R,7aS stereochemistry for **9a**.

On the other hand, the stereochemistry assignment was clearer for **9b**. Analysis of 1D and 2D NOESY experiments allowed us to find strong dipolar correlations between H-7a and both H-4a and the methyl protons at C-7 position that indicated they are all on the same face of the molecule. In addition, medium and weak NOE effects were observed for H-7 and H-1 as well as between H-7 and H-5, respectively; data that together with a strong NOE effect of H-5 with H-4, located all these protons on the opposite face of the molecule. As a result, we now propose the 1S,4aR,5R,7S,7aR stereochemistry for **9b**.

In order to confirm the previously described observations, a conformational search using the same conditions applied for **9a** was undertaken (Fig. 3). The result was also similar, as one major conformational family appeared including the global minimum that was found 65 times. The best energy structure fully reproduces the NMR experimental observations (NOESY and $^3J_{\text{H-H}}$ couplings). This time, the calculated proton–proton coupling constants showed excellent agreement with the experimentally observed values. Therefore, calculated values for $^3J_{\text{H4a-H7a}} = 6.1$ Hz, $^3J_{\text{H7a-H1}} = 2.1$ Hz, $^3J_{\text{H7a-H7}} = 8.3$ Hz, and $^3J_{\text{H4a-H5}} = 1.6$ Hz perfectly matched the experimental ones of $^3J_{\text{H4a-H7a}} = 6.1$ Hz, $^3J_{\text{H7a-H1}} = 2.6$ Hz, and $^3J_{\text{H4a-H5}} \approx 1$ Hz, confirming our proposal.

2.3. Antiproliferative activity

Prior to the synthesis of the compounds reported in this article, we prepared the same set of derivatives but starting from racemic citronellol using the same synthetic strategy described in Scheme 1. In this unreported work, we prepared as a diastereomeric mixture the desilylated derivatives of compounds **9a–b**. The antiproliferative activity of this mixture is listed in Table 1. We observed that the unsilylated bicycle was less active when compared to the silylated precursor. Therefore, for the study reported in our manuscript when we started the synthesis using both enantiomers of citronellol we finished the synthesis with compounds **9a–b**.

The antiproliferative activity of bicyclic analogs **9a–b** was studied using the NCI protocol.¹⁵ The effect, defined as 50% growth inhibition (GI_{50}),¹⁶ was determined against the panel of representative human solid tumor cell lines A2780 (ovarian), HBL-100 (breast), HeLa (cervix), SW1573 (non-small cell lung), T-47D (breast), and WiDr (colon). Compounds **9a–b** showed very active against all cell lines with GI_{50} values in the range 0.38–1.86 μM (Table 1). Interestingly, the data reveals a similar pattern of activity of both stereoisomers.

When comparing the growth inhibition data of the simplified aglycones **9a–b** (Table 1) with those obtained for catalpol (**2**) and its silylated derivatives,⁶ an important consequence can be inferred. The aglycone fragment alone is more potent than when it is attached to a sugar moiety. In fact, catalpol (**2**) showed inactive ($\text{GI}_{50} > 100 \mu\text{M}$) against the same panel of cell lines used in this study.⁶

2.4. Cell cycle disturbances

In addition to growth inhibition, we studied cell cycle phase distribution by flow cytometry to determine if cell growth inhibition involved cell cycle changes. DNA polymerase inhibitors are known to interfere with the cell cycle and cause arrest in G_0/G_1 phase.¹⁷ To study the influence on the cell cycle, we selected HBL-100 and SW1573 cells as representative examples. The cells were exposed

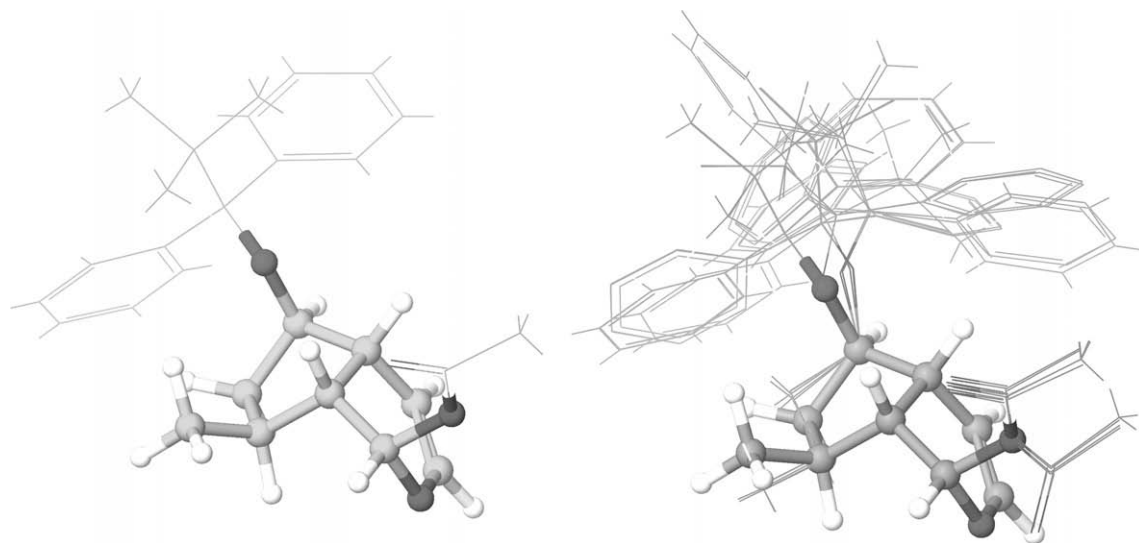
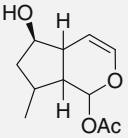


Figure 3. From left to right: Best energy structure found for **9b** and superimposition of the 10 best energy structures found in the conformational search of **9b** ($\Delta E = +6.5$ kJ/mol).

Table 1
Antiproliferative activity (GI_{50}) against human solid tumor cells^a

Cell line	9a	9b	
A2780 (ovarian)	1.24 (± 0.05)	1.59 (± 0.13)	15 (± 0.5)
HBL-100 (breast)	0.38 (± 0.04)	0.50 (± 0.14)	16 (± 1.2)
HeLa (cervix)	1.68 (± 0.31)	1.86 (± 0.07)	n.d. ^b
SW1573 (lung)	0.43 (± 0.02)	0.59 (± 0.11)	18 (± 1.5)
T-47D (breast)	1.62 (± 0.07)	1.46 (± 0.35)	16 (± 1.4)
WiDr (colon)	1.13 (± 0.02)	1.26 (± 0.34)	16 (± 1.8)

^a Values are given in $\mu M \pm$ standard deviation and are means of three to five experiments.

^b n.d. = not done.

to compound **9b** for 24 h at four different doses (1, 2, 3, and 5 μM), which were chosen based on the GI_{50} values of the drug.

The results of cell cycle distributions of samples collected from control and treated cells are summarized in Figure 4. Overall, the same effect is obtained for the cell cycle distribution of HBL-100 and SW1573 cells exposed to analog **9b**. At the low doses 1 and 2 μM , an increase in the percentage of cells in the G_0/G_1 phase was observed. The rise is concomitant with a decrease in the S phase compartment and consistent with DNA polymerase inhibition. The exposure to the higher drug doses 3 and 5 μM induces cell kill in a dose dependent manner, as shown by the appearance of a sub- G_1 peak. Based on the results of cell cycle distribution, we speculate that the sub- G_1 peak originates from cells arrested in G_0/G_1 phase. The percentage of cells in both G_0/G_1 and sub- G_1 phase represent in all drug treatments more than the amount of untreated cells in G_0/G_1 . This implies that compound-induced cell death occurs for those cells arrested in G_0/G_1 phase.

2.5. Annexin V binding

Our next efforts were directed to determine if cell death was occurring through apoptosis. Apoptosis is a highly regulated form of cell death involving multiple signaling pathways that is triggered when a cell has been damaged and cannot recover. Several studies have shown that most, if not all, chemotherapeutic agents

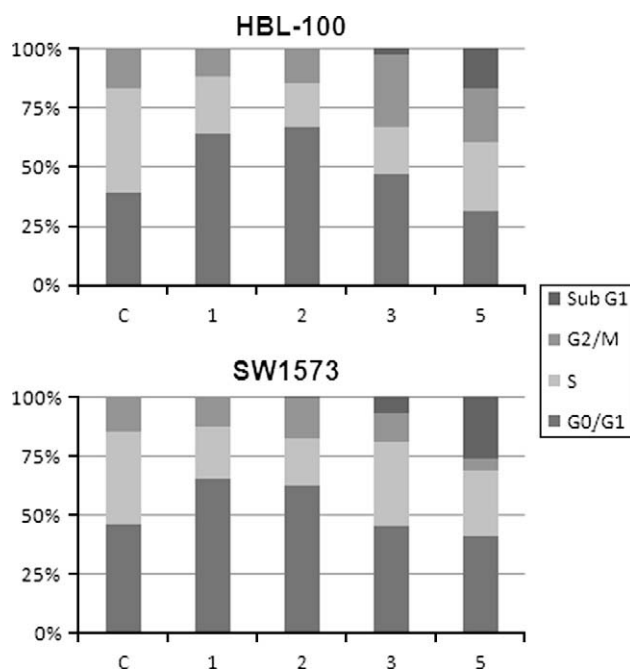


Figure 4. Cell cycle phase distribution of untreated (control) SW1573 and HBL-100 cells, and cells treated with compound **9b** for 24 h at 1, 2, 3, and 5 μM drug dose.

exert their anticancer activity by inducing apoptosis. In the early stages of apoptosis, the phosphatidyl choline residues of the cell membrane are translocated from the inner to the outer membrane surface. The residues can be labeled with Annexin V-FITC and detected by flow cytometry.

To study the induction of apoptosis, we selected HeLa and WiDr cells as representative examples. The cells were exposed to compounds **9a–b** for 24 h at 3 μM . Flow cytometry analysis of samples labeled with Annexin V confirmed that both compounds were able to induce apoptosis (Fig. 5).

2.6. Immunoblotting

In eukaryotic cells, progression of the cell cycle is controlled by checkpoints. One of these checkpoints is cyclin D1, which acts as a

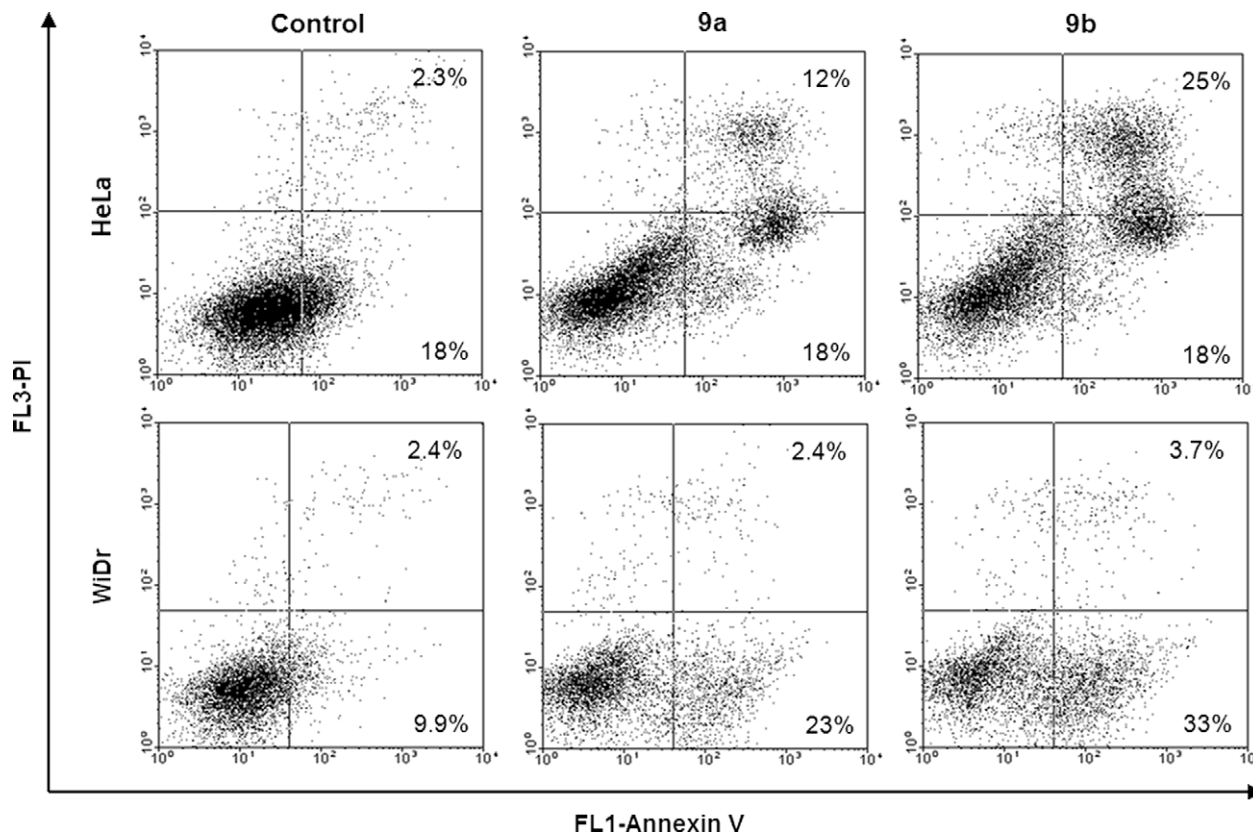


Figure 5. Annexin V and PI staining of untreated cells (Control) and cells treated with compounds **9a–b** for 24 h at 3 μ M drug dose. Viable cells are AnnexinV[−] and PI[−], early apoptotic cells are AnnexinV⁺ and PI[−], and late apoptotic cells are AnnexinV⁺ and PI⁺. Quantification of apoptosis showed the percentage of cells that were apoptotic.

regulator of G₁/S-phase progression.¹⁸ Cyclin D1 levels begin to rise early in G₁ and continue to accumulate until the G₁/S-phase boundary when levels rapidly decline. Immunoblotting of HeLa cells exposed to **9b** reduced cyclin D1 levels in a time dependent manner (Fig. 6). This result is consistent with the observed cell cycle arrest on G₁ (Fig. 4).

In summary, we have synthesized a bicyclic derivative by means of a cyclization catalyzed by L-proline. The title compound represents a simplified scaffold of the aglycone framework of naturally occurring iridoids. These compounds show remarkable biological activity towards human cancer cell lines, including cell cycle arrest and apoptosis induction. More experiments are ongoing to corroborate the scope of these simplified analogs as potential therapeutics for the treatment of cancer, either alone or in combination.

3. Experimental

3.1. General

Reactions requiring anhydrous conditions were performed under nitrogen. Dichloromethane and ethyl ether were distilled

from CaH₂ and Na/benzophenone, respectively, under N₂ prior to use. Other solvents or chemicals were purified by standard techniques.¹⁹ Thin-layer chromatography was carried out on Merck aluminium sheets coated with Silica Gel 60 F₂₅₄. Plates were visualized by use of UV light and/or phosphomolybdic acid 20wt % solution in ethanol with heating. Anhydrous magnesium sulfate was used for drying solutions. Flash chromatography was performed on Silica Gel Merck grade 9385, 60 Å. Optical rotations were determined for solutions in chloroform on a Perkin Elmer 343 polarimeter. NMR spectra were measured at 500, 400 or 300 MHz (¹H NMR) and 75 MHz (¹³C NMR), and chemical shifts are reported relative to internal Me₄Si (δ = 0). IR spectra were recorded on a Bruker IFS 55 spectrometer model.

3.1.1. (R)-3,7-Dimethyloct-6-enyl benzoate (**4a**)

To a solution of (+)- β -citronellol (**3a**) (2.95 g, 18.87 mmol) in dry CH₂Cl₂ (188 mL) under argon atmosphere were sequentially added Et₃N (3.9 mL, 28.3 mmol) and benzoyl chloride (2.6 mL, 22.65 mmol) at 0 °C. The reaction was stirred for 2 h, after which time TLC showed that the starting material had disappeared. Then saturated aqueous solution of NaCl was added and the resulting mixture was extracted with CH₂Cl₂. The combined organic phases were dried, filtered, and evaporated in vacuum. The residue was purified by column chromatography on silica gel to give **4a** (4.86 g, 99% yield) as a colorless oil: $[\alpha]_D^{20}$ = +3.47 (*c* 3.8 in CHCl₃); ¹H NMR (300 MHz, CDCl₃) δ (ppm): 0.97 (d, *J* = 6.3 Hz, 3H), 1.20–1.29 (m, 1H), 1.35–1.46 (m, 1H), 1.54–1.85 (m, 9H), 1.96–2.06 (m, 2H), 4.32–4.38 (m, 2H), 5.10 (dd, *J* = 6.9, 6.9 Hz, 1H), 7.40–7.45 (m, 2H), 7.52–7.56 (m, 1H), 8.03–8.05 (m, 2H); ¹³C NMR (75 MHz, CDCl₃) δ : 17.4 (q), 19.2 (q), 25.1 (t), 25.4 (q), 29.2 (d), 35.2 (t), 36.7 (t), 63.2 (t), 124.3 (d), 128.0 (d), 129.2 (d), 130.2 (s), 131.1 (s), 132.5 (d), 166.4 (s); IR (film) ν cm^{−1} 2962, 2958, 1721,

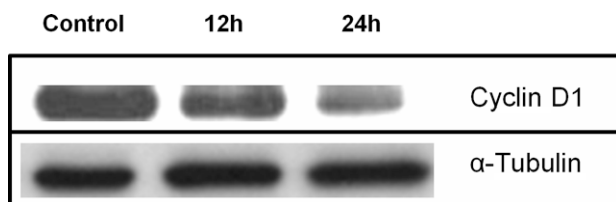


Figure 6. Western blot analysis of protein extracts from HeLa cells exposed to compound **9b** at 10 μ M after 12 and 24 h of drug treatment.

1273, 1112, 711; MS (EI+) m/z (%): 138 (72) $[M-BzOH]^+$, 123 (66), 123 (75), 109 (26), 105 (100), 95 (61); HRMS-EI m/z $[M-BzOH]^+$ calcd for $C_{10}H_{18}$: 138.1409, found: 138.1404.

3.1.2. (S)-3,7-Dimethyloct-6-enyl benzoate (4b)

The procedure used above to obtain **4a** from (+)- β -citronellol (**3a**) was applied to (–)- β -citronellol (**3b**) on a 4.9 g (31.35 mmol) scale, yielding **4b** (8.08 g, 99% yield) as a colorless oil: $[\alpha]_D^{20} = -3.19$ (c 3.7 in $CHCl_3$); 1H NMR (300 MHz, $CDCl_3$), δ (ppm): 0.97 (d, $J = 6.4$ Hz, 3H), 1.20–1.30 (m, 1H), 1.35–1.70 (m, 9H), 1.77–1.86 (m, 1H), 1.96–2.06 (m, 2H), 4.32–4.39 (m, 2H), 5.10 (dd, $J = 7.0$, 7.0 Hz, 1H), 7.40–7.45 (m, 2H), 7.52–7.57 (m, 1H), 8.02–8.05 (m, 2H); ^{13}C NMR (75 MHz, $CDCl_3$): δ 17.4 (q), 19.2 (q), 25.1 (t), 25.4 (q), 29.3 (d), 35.2 (t), 36.7 (t), 63.2 (t), 124.3 (d), 128.0 (d), 129.2 (d), 130.2 (s), 131.1 (s), 132.5 (d), 166.4 ppm (s); IR (film) ν cm^{-1} 2962, 2920, 1721, 1274, 1112, 711; MS (EI+) m/z (%): 261 (0.2) $[M+1]^+$, 138 (63) $[M-BzOH]^+$, 123 (66), 109 (23), 105 (100), 95 (56); HRMS-EI m/z $[M]^+$ calcd for $C_{17}H_{24}O_2$: 260.1779, found: 260.1776.

3.1.3. (R)-5-Formyl-3-methylpentyl benzoate (5a)

A solution of **4a** (4.46 g, 17.15 mmol) and pyridine (2.1 mL, 25.72 mmol) in CH_2Cl_2 /MeOH (77 mL/8.5 mL) was cooled to $-78^\circ C$. Ozone was bubbled through the solution until a dark blue color developed. At this time triphenylphosphine (5.0 g, 18.86 mmol) was added and the resulting mixture was stirred for 3 h allowing it to reach $0^\circ C$. After concentration, flash chromatography (Hexanes/AcOEt = 95:5) afforded the title compound as a clear, colorless oil in 95% yield (3.8 g): $[\alpha]_D^{20} = +3.13$ (c 4.1 in $CHCl_3$); 1H NMR (300 MHz, $CDCl_3$), δ (ppm): 0.93 (d, $J = 6.1$ Hz, 3H), 1.41–1.81 (m, 5H), 2.31–2.49 (m, 2H), 4.33 (ddd, $J = 6.3$, 6.3, 3.1 Hz, 2H), 7.36–7.41 (m, 2H), 7.48–7.53 (m, 1H), 7.97–8.00 (m, 2H), 9.72 (s, 1H); ^{13}C NMR (75 MHz, $CDCl_3$): δ 18.8 (q), 28.4 (t), 29.3 (d), 35.0 (t), 41.2 (t), 62.8 (t), 128.1 (d), 129.2 (d), 130.0 (s), 132.5 (d), 166.3 (s), 202.1 (d); IR (film): ν cm^{-1} 2960, 2930, 2361, 2338, 1719, 1275, 1112, 713; MS (EI+) m/z (%) 233 (0.2) $[M-1]^+$, 128 (95), 123 (32), 122 (10), 110 (42), 105 (100); HRMS-EI m/z $[M-1]^+$ calcd for $C_{14}H_{17}O_3$: 233.1178, found: 233.1172.

3.1.4. (S)-5-Formyl-3-methylpentyl benzoate (5b)

The procedure used above to obtain **5a** from **4a** was applied to **4b** on a 8.0 g (30.72 mmol) scale, yielding **5b** (6.9 g, 96% yield) as a colorless oil: $[\alpha]_D^{20} = -3.09$ (c 4.1 in $CHCl_3$); 1H NMR (300 MHz, $CDCl_3$), δ (ppm): 0.93 (d, $J = 6.1$ Hz, 3H), 1.44–1.78 (m, 5H), 2.31–2.43 (m, 2H), 4.29–4.34 (m, 2H), 7.35–7.40 (m, 2H), 7.46–7.51 (m, 1H), 7.97–8.00 (m, 2H), 9.71 (s, 1H); ^{13}C NMR (75 MHz, $CDCl_3$): δ 18.8 (q), 28.4 (t), 29.3 (d), 35.0 (t), 41.2 (t), 62.8 (t), 128.0 (d), 129.2 (d), 130.0 (s), 132.6 (d), 166.3 (s), 202.2 (d); IR (film): ν cm^{-1} 2960, 2361, 1716, 1276, 1112, 713; MS (EI+) m/z (%) 233 (0.2) $[M-1]^+$, 128 (86), 123 (32), 105 (100); HRMS-EI m/z $[M-1]^+$ calcd for $C_{14}H_{17}O_3$: 233.1178, found: 233.1165.

3.1.5. (E,3S,5R)-7-(Methoxycarbonyl)-5-hydroxy-3-methylhept-6-enyl benzoate (6a)

L-Proline (0.71 g, 6.16 mmol) was added to a stirring solution of **5a** (3.6 g, 15.40 mmol) and nitrosobenzene (1.7 g, 15.40 mmol) in DMSO (62 mL). After 0.5 h the solution became a bright orange, at which time it was cooled to $-15^\circ C$. A premixed solution of methyl diethyl phosphonoacetate (7.5 mL, 46.22 mmol), 1,8-diazabicyclo[5.4.0]undec-7-ene (7 mL, 46.22 mmol) and lithium chloride (1.96 g, 46.22 mmol) in CH_3CN (62 mL) was added over 5 min via cannula. After 15 min the solution was diluted with MeOH (204 mL) and NH_4Cl (2.47 g, 46.22 mmol) was added. The resulting mixture was allowed to warm to room temperature and stand for 2 d. At this time the solution was diluted with Et_2O (1000 mL), and washed successively with saturated solutions of

NH_4Cl , $NaHCO_3$, and $NaCl$. The aqueous layers were extracted with CH_2Cl_2 , and the combined organic layers were dried over $MgSO_4$ and concentrated in vacuum. Flash chromatography (Hexanes/AcOEt = 9:1–6:4) afforded 1.13 g of **6a** as oil (24% yield): $[\alpha]_D^{20} = +16.5$ (c 2.0 in $CHCl_3$); 1H NMR (300 MHz, $CDCl_3$), δ (ppm): 1.00 (d, $J = 6.5$ Hz, 3H), 1.37 (ddd, $J = 13.5$, 9.3, 4.0 Hz, 1H), 1.59–1.68 (m, 2H), 1.73–1.84 (m, 1H), 1.87–1.94 (m, 1H), 2.43 (br s, 1H), 3.70 (s, 3H), 4.27–4.43 (m, 3H), 6.03 (d, $J = 15.6$ Hz, 1H), 6.94 (dd, $J = 15.6$, 4.7 Hz, 1H), 7.33–7.43 (m, 2H), 7.50–7.55 (m, 1H), 7.99–8.01 (m, 2H); ^{13}C NMR (75 MHz, $CDCl_3$): δ 18.8 (q), 26.1 (d), 35.8 (t), 43.3 (t), 51.4 (q), 62.8 (t), 68.5 (d), 119.2 (d), 128.1 (d), 129.3 (d), 129.9 (s), 132.7 (d), 150.2 (d), 166.5 (s), 166.8 (s); IR (film): ν cm^{-1} 3490, 2957, 1718, 1452, 1276, 1115, 714; MS (EI+) m/z (%): 274 (1) $[M-CH_3OH]^+$, 256 (2), 184 (3), 166 (9), 123 (20), 122 (10), 107 (13), 105 (100), 92 (33); HRMS-EI m/z $[M-CH_3OH]^+$ calcd for $C_{16}H_{18}O_4$: 274.1205, found: 274.1210.

3.1.6. (E,3R,5R)-7-(Methoxycarbonyl)-5-hydroxy-3-methylhept-6-enyl benzoate (6b)

The procedure used above to obtain **6a** from **5a** was applied to **5b** on a 6.8 g (28.93 mmol) scale, yielding **6b** (2.1 g, 24% yield) as oil: $[\alpha]_D^{20} = -10.69$ (c 2.1 in $CHCl_3$); 1H NMR (300 MHz, $CDCl_3$), δ (ppm): 1.02 (d, $J = 6.6$ Hz, 3H), 1.53–1.61 (m, 3H), 1.84–1.91 (m, 2H), 2.14 (br s, 1H), 3.71 (s, 3H), 4.29–4.43 (m, 3H), 6.0 (dd, $J = 15.6$, 1.5 Hz, 1H), 6.94 (dd, $J = 15.6$, 5.1 Hz, 1H), 7.39–7.44 (m, 2H), 7.51–7.57 (m, 1H), 7.99–8.02 (m, 2H); ^{13}C NMR (75 MHz, $CDCl_3$): δ 19.8 (q), 26.4 (d), 34.7 (t), 43.4 (t), 51.4 (q), 62.8 (t), 68.9 (d), 119.5 (d), 128.1 (d), 129.2 (d), 130.0 (s), 132.7 (d), 150.2 (d), 166.4 (s), 166.6 (s); IR (film): ν cm^{-1} 3477, 2956, 2927, 1718, 1452, 1276, 1115, 714; MS (EI+) m/z (%): 274 (4) $[M-CH_3OH]^+$, 184 (4) $[M-BzOH]^+$, 152 (12), 123 (34), 122 (10), 105 (100), 92 (16); HRMS-EI m/z $[M-BzOH]^+$ calcd for $C_{10}H_{16}O_3$: 184.1099, found: 184.1098.

3.1.7. (E,3S,5R)-5-(tert-Butyl-diphenyl-silanyloxy)-7-methoxycarbonyl-3-methyl-6-heptenyl benzoate (7a)

To a stirred solution of the alcohol **6a** (1.0 g, 3.26 mmol) in dry CH_2Cl_2 (32 mL) under nitrogen were added imidazole (673 mg, 9.79 mmol) and *tert*-butylchlorodiphenylsilane (1.3 mL, 4.89 mmol) at $0^\circ C$. The reaction was allowed to warm to room temperature and was stirred overnight. Then it was poured into H_2O and extracted with CH_2Cl_2 . The combined organic phases were washed with saturated solutions of $NaCl$, dried, filtered, and concentrated. The crude obtained was purified by flash chromatography yielding **7b** (1.67 g, 94% yield) as an oil: $[\alpha]_D^{20} = +17.82$ (c 1.7 in $CHCl_3$); 1H NMR (300 MHz, $CDCl_3$), δ (ppm): 0.74 (d, $J = 6.1$ Hz, 3H), 1.05 (s, 9H), 1.25–1.34 (m, 2H), 1.58–1.69 (m, 3H), 3.68 (s, 3H), 4.19 (dd, $J = 6.3$, 6.3 Hz, 2H), 4.35–4.37 (m, 1H), 5.83 (d, $J = 15.6$ Hz, 1H), 6.88 (dd, $J = 15.6$, 5.8 Hz, 1H), 7.30–7.44 (m, 7H), 7.52–7.72 (m, 6H), 7.97–8.00 (m, 2H); ^{13}C NMR (75 MHz, $CDCl_3$): δ 19.1 (s), 19.4 (q), 25.8 (d), 26.3 (q), 26.8 (q), 35.3 (t), 44.7 (t), 51.3 (d), 62.7 (t), 70.8 (d), 119.6 (d), 127.3 (d), 127.4 (d), 128.1 (d), 129.3 (d), 129.5 (d), 129.6 (d), 130.1 (s), 132.6 (d), 133.1 (s), 133.4 (s), 134.6 (d), 135.6 (d), 135.7 (d), 150.1 (d), 166.3 (s), 166.6 (s); IR (film): ν cm^{-1} 3508, 2956, 2932, 2857, 1721, 1274, 1110, 706; MS (EI+) m/z (%): 514 (0.3) $[M-2Me]^+$, 513 (0.8), 488 (14), 487 (39) $[M-tBu]^+$, 304 (25), 303 (100), 243 (37), 199 (19), 135 (14); HRMS-EI m/z $[M-tBu]^+$ calcd for $C_{29}H_{31}O_5Si$: 487.1941, found: 487.1949.

3.1.8. (E,3R,5R)-5-(tert-Butyl-diphenyl-silanyloxy)-7-methoxycarbonyl-3-methyl-6-heptenyl benzoate (7b)

The procedure used above to obtain **7a** from **6a** was applied to **6b** on a 2.0 g (6.52 mmol) scale, yielding **7b** (3.34 g, 94% yield) as oil: $[\alpha]_D^{20} = +9.26$ (c 1.4 in $CHCl_3$); 1H NMR (300 MHz, $CDCl_3$), δ (ppm): 0.68 (d, $J = 4.7$ Hz, 3H), 1.06 (s, 9H), 1.39–1.48 (m, 2H),

1.54–1.61 (m, 3H), 3.68 (s, 3H), 4.19 (d, $J = 6.8$ Hz, 2H), 4.37 (br s, 1H), 5.88 (d, $J = 15.6$ Hz, 1H), 6.89 (dd, $J = 15.6, 5.5$ Hz, 1H), 7.34–7.44 (m, 8H), 7.52–7.72 (m, 5H), 7.97–7.99 (m, 2H); ^{13}C NMR (75 MHz, CDCl_3): δ 18.7 (s), 25.8 (d), 26.3 (q), 26.7 (q), 35.6 (t), 44.2 (t), 51.3 (q), 62.7 (t), 70.7 (d), 119.7 (d), 127.3 (d), 127.4 (d), 127.4 (d), 128.1 (d), 129.2 (d), 129.4 (d), 129.5 (d), 129.6 (d), 130.0 (s), 132.6 (d), 133.0 (s), 133.4 (s), 134.5 (d), 135.6 (d), 149.7 (d), 166.3 (s), 166.6 (s); IR (film): ν cm^{-1} 3476, 2956, 2931, 1721, 1275, 1111, 705; MS (EI+) m/z (%): 487 (41) $[\text{M}-t\text{Bu}]^+$, 304 (24), 303 (98), 243 (36), 135 (17), 105 (100); HRMS-EI m/z $[\text{M}-t\text{Bu}]^+$ calcd for $\text{C}_{29}\text{H}_{31}\text{O}_5\text{Si}$: 487.1941, found: 487.1935.

3.1.9. (E,4R,6S)-6-Methyl-4-(*tert*-butyl-diphenyl-silanyloxy)-2-octene-1,8-diol (**8a**)

To a cooled solution of the compound **7a** (358 mg, 0.65 mmol) in dry Et_2O (6.5 mL) under argon atmosphere was added dropwise DIBAL-H (3.9 mL 1 M in cyclohexane, 3.94 mmol) at -78°C . The mixture was stirred at -78°C until no starting material was presented by TLC. The reaction was quenched by the addition of 0.1 mL of H_2O and then, to the same flask, was added MgSO_4 . The gelatinous solution was filtered through a pad of Celite and washed with Et_2O . The solvent was removed under reduced pressure, and the residue was purified by flash chromatography on a silica gel column yielding **8a** (122 mg, 45% yield) as a colorless oil: $[\alpha]_D^{20} = +13.05$ (c 1.6 in CHCl_3); ^1H NMR (300 MHz, CDCl_3): δ (ppm): 0.77 (d, $J = 6.5$ Hz, 3H), 1.04 (s, 9H), 1.17–1.32 (m, 2H), 1.36–1.49 (m, 2H), 1.53–1.78 (m, 3H), 3.54 (m, 2H), 3.86 (d, $J = 5.5$ Hz, 2H), 4.23 (dd, $J = 13.2, 6.6$ Hz, 1H), 5.37 (ddd, $J = 15.4, 11.0, 5.5$ Hz, 1H), 5.55 (dd, $J = 15.4, 7.2$ Hz, 1H), 7.32–7.45 (m, 6H), 7.63–7.69 (m, 4H); ^{13}C NMR (75 MHz, CDCl_3): δ 19.0 (s), 19.8 (q), 25.2 (d), 26.8 (q), 39.48 (t), 45.1 (t), 60.5 (t), 62.7 (t), 72.0 (d), 127.0 (d), 127.2 (d), 129.1 (d), 129.2 (d), 129.4 (d), 133.9 (s), 134.2 (s), 134.5 (d), 135.7 (d), 135.8 (d); IR (film): ν cm^{-1} 3382, 2931, 1645, 1427, 1109, 1059, 740, 703; MS (EI+) m/z (%): 337 (32) $[\text{M}-t\text{Bu}-\text{H}_2\text{O}]^+$, 325 (3), 200 (19), 199 (100), 197 (11), 139 (18); HRMS-EI m/z $[\text{M}-t\text{Bu}-\text{H}_2\text{O}]^+$ calcd for $\text{C}_{21}\text{H}_{25}\text{O}_2\text{Si}$: 337.1624, found: 337.1615.

3.1.10. (E,4R,6R)-6-Methyl-4-(*tert*-butyl-diphenyl-silanyloxy)-2-octene-1,8-diol (**8b**)

The procedure used above to obtain **8a** from **7a** was applied to **7b** on a 1.6 g (2.99 mmol) scale, yielding **8b** (545 mg, 45% yield) as a colorless oil: $[\alpha]_D^{20} = +0.27$ (c 3.6 in CHCl_3); ^1H NMR (300 MHz, CDCl_3): δ (ppm): 0.67 (d, $J = 6.2$ Hz, 3H), 1.05 (s, 9H), 1.20–1.29 (m, 1H), 1.32–1.47 (m, 4H), 1.68 (br s, 2H), 3.56 (ddd, $J = 17.0, 10.6, 6.5$ Hz, 2H), 3.89 (d, $J = 5.4$ Hz, 2H), 4.19 (dd, $J = 13.0, 7.3$ Hz, 1H), 5.38 (ddd, $J = 15.4, 11.0, 5.4$ Hz, 1H), 5.55 (dd, $J = 15.4, 7.3$ Hz, 1H), 7.32–7.43 (m, 6H), 7.63–7.68 (m, 4H); ^{13}C NMR (75 MHz, CDCl_3): δ 19.0 (s), 19.4 (q), 25.2 (d), 26.7 (q), 39.8 (t), 45.0 (t), 60.3 (t), 62.6 (t), 72.3 (d), 127.1 (d), 127.2 (d), 129.2 (d), 129.3 (d), 129.4 (d), 134.0 (s), 134.1 (d), 134.2 (s), 135.7 (d), 135.8 (d); IR (film): ν cm^{-1} 3391, 2930, 2360, 1646, 1427, 1109, 822, 703; MS (EI+) m/z (%): 337 (14) $[\text{M}-t\text{Bu}-\text{H}_2\text{O}]^+$, 335 (3), 323 (3), 239 (1), 200 (17), 199 (100), 139 (11); HRMS-EI m/z $[\text{M}-t\text{Bu}-\text{H}_2\text{O}]^+$ calcd for $\text{C}_{21}\text{H}_{25}\text{O}_2\text{Si}$: 337.1624, found: 337.1622.

3.1.11. (1R,4aS,5R,7R,7aS)-5-(*tert*-Butyl-diphenyl-silanyloxy)-7-methyl-1,4a,5,6,7,7a-hexahydrocyclopenta[c]pyran-1-yl acetate (**9a**)

Dess–Martin periodinane (194 mg, 0.46 mmol) was added to a stirred solution of **8a** (82 mg, 0.20 mmol) in CH_2Cl_2 (2 mL). After 40 min the reaction was concentrated and extracted with pentane. The combined organics were concentrated in vacuum, providing the corresponding dialdehyde, which was immediately redissolved in DMSO (5 mL). L-proline (7 mg, 0.06 mmol) was added to this stirred solution in one portion. After 5 h, the reaction was warmed

to 40°C and stirred at this temperature for 60 h. The reaction was then cooled to 0°C , and acetic anhydride (0.17 mL, 1.79 mmol) was added, followed by pyridine (0.07 mL, 0.91 mmol) and DMAP (2 mg, 0.01 mmol). After 15 min the reaction was diluted with Et_2O and washed with saturated solutions of NH_4Cl , NaHCO_3 , and NaCl . The aqueous layers were then extracted with CH_2Cl_2 and Et_2O . The combined organic layers were dried over MgSO_4 and concentrated in vacuum. Flash chromatography (Hexanes/ $\text{AcOEt} = 98:2$) afforded **9a** as a clear, colorless oil in 15% yield (13 mg): $[\alpha]_D^{20} = +80.44$ (c 1.2 in CHCl_3); ^1H NMR (500 MHz, CDCl_3): δ (ppm): 0.85 (d, $J = 6.8$ Hz, 3H, CHCH_3), 1.09 (s, 9H, $t\text{Bu}$), 1.67 (ddd, $J = 7.3, 7.3, 4.1$ Hz, 1H, H_{7a}), 1.85–1.90 (m, 2H, $2 \times \text{H}_6$), 2.10 (br s, 4H, H_7 , OCOCH_3), 2.58 (ddd, $J = 7.6, 5.2, 2.5$ Hz, 1H, H_{4a}), 4.25 (ddd, $J = 6.6, 6.6, 1.8$ Hz, 1H, H_5), 5.04 (dd, $J = 6.4, 2.6$ Hz, 1H, H_4), 6.07 (d, $J = 4.2$ Hz, 1H, H_1), 6.33 (dd, $J = 6.3, 2.2$ Hz, 1H, H_3), 7.38–7.45 (m, 6H, Ar), 7.52–7.68 (m, 4H, Ar); ^{13}C NMR (75 MHz, CDCl_3): δ 19.0 (s, $t\text{Bu}$), 20.9 (q, OCOCH_3), 21.0 (q, CHCH_3), 26.6 (q, $t\text{Bu}$), 31.1 (d, C_7), 38.3 (d, C_{4a}), 40.4 (t, C_6), 45.5 (d, C_{7a}), 74.8 (d, C_5), 91.1 (d, C_1), 100.8 (d, C_4), 127.3 (d, Ar), 127.3 (d, Ar), 129.4 (d, Ar), 133.6 (s, Ar), 133.9 (s, Ar), 135.5 (d, Ar), 135.6 (d, Ar), 140.5 (d, C_3), 169.8 (s, OCOCH_3); IR (film): ν cm^{-1} 3446, 2928, 2856, 1750, 1650, 1211, 1110, 703, 505 cm^{-1} ; MS (EI+) m/z (%): 393 (4) $[\text{M}-t\text{Bu}]^+$, 333 (40) $[\text{M}-t\text{Bu}-\text{AcOH}]^+$, 319 (16), 245 (10), 241 (26), 199 (100), 181 (13); HRMS-EI m/z $[\text{M}-t\text{Bu}-\text{AcOH}]^+$ calcd for $\text{C}_{21}\text{H}_{21}\text{O}_2\text{Si}$: 333.1311, found: 333.1297.

3.1.12. (1S,4aR,5R,7S,7aR)-5-(*tert*-Butyl-diphenyl-silanyloxy)-7-methyl-1,4a,5,6,7,7a-hexahydrocyclopenta[c]pyran-1-yl acetate (**9b**)

The procedure used above to obtain **9a** from **8a** was applied to **8b** on a 247 mg (0.59 mmol) scale, yielding **9b** (40 mg, 15% yield) as a colorless oil: $[\alpha]_D^{20} = -76.45$ (c 1.1 in CHCl_3); ^1H NMR (500 MHz, CDCl_3): δ (ppm): 1.00 (s, 9H, $t\text{Bu}$), 1.14 (d, $J = 6.7$ Hz, 3H, CHCH_3), 1.91 (dddd, $J = 13.6, 6.8, 6.8, 2.2$ Hz, 1H, H_7), 2.04–2.15 (m, 6H, H_{7a} , $2 \times \text{H}_6$, OCOCH_3), 2.62 (d, $J = 6.0$ Hz, 1H, H_{4a}), 4.00 (dd, $J = 5.4, 3.1$ Hz, 1H, H_5), 4.34 (ddd, $J = 6.3, 2.5, 1.1$ Hz, 1H, H_4), 6.02 (dd, $J = 6.3, 2.3$ Hz, 1H, H_3), 6.09 (d, $J = 2.6$ Hz, 1H, H_1), 7.38–7.47 (m, 6H, Ar), 7.67–7.69 (m, 4H, Ar); ^{13}C NMR (75 MHz, CDCl_3): δ 18.8 (s, $t\text{Bu}$), 20.4 (q, CHCH_3), 21.0 (q, OCOCH_3), 26.6 (q, $t\text{Bu}$), 32.8 (d, C_7), 41.2 (d, C_{4a}), 42.1 (t, C_6), 45.8 (d, C_{7a}), 79.1 (d, C_5), 90.1 (d, C_1), 103.2 (d, C_4), 127.3 (d, Ar), 129.4 (d, Ar), 133.7 (s, Ar), 133.9 (s, Ar), 135.4 (d, Ar), 135.5 (d, Ar), 139.4 (d, C_3), 170.1 (s, OCOCH_3); IR (film): ν cm^{-1} 3450, 2957, 2930, 2857, 1750, 1654, 1215, 1110, 703, 507; MS (EI+) m/z (%) 393 (4) $[\text{M}-t\text{Bu}]^+$, 351 (3) $[\text{M}-t\text{Bu}-\text{Ac}+1]^+$, 334 (10), 333 (37) $[\text{M}-t\text{Bu}-\text{AcOH}]^+$, 319 (16), 315 (11), 255 (10), 199 (100); HRMS-EI m/z $[\text{M}-t\text{Bu}-\text{AcOH}]^+$ calcd for $\text{C}_{21}\text{H}_{21}\text{O}_2\text{Si}$: 333.1311, found: 333.1287.

3.2. Biological tests

All starting materials were commercially available research-grade chemicals and used without further purification. RPMI 1640 medium was purchased from Flow Laboratories (Irvine, UK), fetal calf serum (FCS) was from Gibco (Grand Island, NY), trichloroacetic acid (TCA) and glutamine were from Merck (Darmstadt, Germany), and penicillin G, streptomycin, dimethyl sulfoxide (DMSO), and sulforhodamine B (SRB) were from Sigma (St Louis, MO).

3.2.1. Cells, culture and plating

The human solid tumor cell lines A2780, HBL-100, HeLa, SW1573, T-47D, and WiDr were used in this study. These cell lines were a kind gift from Professor Godefridus J. Peters (VU Medical Center, Amsterdam, The Netherlands). Cells were maintained in 25 cm^2 culture flasks in RPMI 1640 supplemented with 5% heat inactivated fetal calf serum and 2 mM L-glutamine in a 37°C , 5%

CO₂, 95% humidified air incubator. Exponentially growing cells were trypsinized and resuspended in antibiotic containing medium (100 units penicillin G and 0.1 mg of streptomycin per mL). Single cell suspensions displaying >97% viability by trypan blue dye exclusion were subsequently counted. After counting, dilutions were made to give the appropriate cell densities for inoculation onto 96-well microtiter plates. Cells were inoculated in a volume of 100 µL per well at densities of 15,000 (WiDr, T-47D and HeLa) and 10,000 (A2780, SW1573 and HBL-100) cells per well, based on their doubling times.

3.2.2. Antiproliferative tests

Chemosensitivity tests were performed using the SRB assay of the NCI with slight modifications. Briefly, pure compounds were initially dissolved in DMSO at 400 times the desired final maximum test concentration. Control cells were exposed to an equivalent concentration of DMSO (0.25% v/v, negative control). Each agent was tested in triplicates at different dilutions in the range 1–100 µM. The drug treatment was started on day 1 after plating. Drug incubation times were 48 h, after which time cells were precipitated with 25 µL ice-cold 50% (w/v) trichloroacetic acid and fixed for 60 min at 4 °C. Then the SRB assay was performed. The optical density (OD) of each well was measured at 492 nm, using BioTek's PowerWave XS Absorbance Microplate Reader. Values were corrected for background OD from wells only containing medium. The percentage growth (PG) was calculated with respect to untreated control cells (C) at each of the drug concentration levels based on the difference in OD at the start (T_0) and end of drug exposure (T), according to NCI formulas. Therefore, if T is greater than or equal to T_0 the calculation is $100 \times [(T - T_0)/(C - T_0)]$. If T is less than T_0 denoting cell killing the calculation is $100 \times [(T - T_0)/(T_0)]$. The effect is defined as percentage of growth, where 50% growth inhibition (GI_{50}) represents the concentration at which PG is +50. With these calculations a PG value of 0 corresponds to the amount of cells present at the start of drug exposure, while negative PG values denote net cell kill.

3.2.3. Cell cycle analysis

Cells were seeded in a six well plates at a density of $2.5\text{--}5 \times 10^5$ cells/well. After 24 h the products were added to the respective well and incubated for an additional period of 24 h. Cells were trypsinized, harvested, transferred to test tubes (12 × 75 mm) and centrifuged at 1,500 rpm for 10 minutes at 5 °C. The supernatant was discarded and the cell pellets were resuspended in 200 µL of cold PBS and fixed by the addition of 1 mL ice-cold 70% ethanol. Fixed cells were incubated overnight at –20 °C after which time was centrifuged at 1,500 rpm for 10 minutes. The cell pellets were resuspended in 500 µL PBS. Then, 5 µL of DNase-free RNase (10 mg/mL) was incubated in the dark at 37 °C for 30 minutes. After incubation 5 µL of propidium iodide (0.5%) was added. Flow cytometric determination of DNA content (25,000 cells/sample) was analyzed by LSR II Flow Cytometer (Becton Dickinson, San José, CA, USA). The fractions of the cells in sub G_1 , G_0/G_1 , S, and G_2/M phase were analyzed using cell cycle analysis software, FACS-Diva 6.0 (Becton Dickinson, San José, CA, USA).

3.2.4. Annexin V binding

Cells were seeded in six well plates at a density of $0.25\text{--}0.5 \times 10^6$ cells. After 24 h, the test drug was added and the cells incubated for period of 24 h. Then, the medium was removed and substituted by drug-free fresh medium. Cells were incubated for an additional period of 24 h. Then, cells were trypsinized, harvested, transferred to test tubes (12 × 75 mm) and centrifuged at 400 g for 10 min. The supernatant was discarded and the cells pellets were resuspended in 100 µL of ice-cold 1x binding buffer (0.1 M Hepes/NaOH (pH 7.4) 1.4 M NaCl, 25 mM CaCl₂).

Annexin staining protocol was performed according to the manufacturer's protocol (Annexin V-FITC apoptosis detection Kit I, Becton Dickinson, San José, CA), with minor modifications. Cells were stained by the addition of both 5 µL Annexin V-FITC and 5 µL PI solution. Samples were gently vortexed and incubated for 15 min at rt. in the dark. Then, 400 µL of 1x binding buffer was added to each tube. The samples were analyzed by flow cytometry using Cell Quest Pro software (Becton Dickinson, San José, CA). Typically, 10,000 events were collected using excitation/emission wavelengths of 488/525 and 488/675 nm for Annexin V and PI, respectively. Results were processed using WinMDI 2.8 free software.

3.2.5. Immunoblotting

Protein extracts were prepared using a lysis buffer freshly supplemented with protease and phosphatase inhibitors [50 mM Tris (pH 8.0), 250 mM NaCl, 1% NP-40, 0.1% SDS, 5 mM EDTA, 2 mM Na₃VO₄, 10 mM Na₂P₂O₇, 10 mM NaF, 10 µg/mL aprotinin, 10 µg/mL leupeptin, 0.5 µg/mL pepstatin, and 1 mM PMSF]. Cells were incubated on ice for 10 min and then cell debris was spun down at 10,000g for 10 min. Proteins were separated by SDS-PAGE and electrotransferred to ImmunoBlot PVDF membrane (BioRad). Cyclin D1 (Santa Cruz, USA) primary antibody was used. After being washed with TBST, membranes were incubated with horseradish peroxidase-conjugated secondary antibodies for 30 min and bands were visualized by a luminal-based detection system with *p*-iodophenol enhancement.

Acknowledgments

This research was supported by the Spanish MEC co-financed by the European Regional Development Fund (CTQ2008-06806-C02-01/BQU), and the Canary Islands ACIISI (PI 2007/021) co-financed by the European FEDER; the Spanish MSC (RTICC RD06/0020/1046 and RD06/0020/0041) and FUNCIS (REDEFAC PI 01/06 and 35/06); the Argentinian UNSL (22/Q505), CONICET (PIP 6228) and AN-PCyT (PICT-10714, 9759). C.R.P. and C.E.T. belong to CIC-CONICET. L.G.L. thanks the Spanish MSC-FIS for a postdoctoral contract. C.G. and J.M.P. thank the Spanish MEC-FSE for Ramón y Cajal contracts.

Supplementary data

Supplementary data associated with this article can be found, in the online version, at [doi:10.1016/j.bmc.2010.02.044](https://doi.org/10.1016/j.bmc.2010.02.044).

References and notes

- (a) Tan, G.; Gyllenhaal, C.; Soejarto, D. D. *Curr. Drug Targets* **2006**, *7*, 265; (b) Pezzuto, J. M. *Biochem. Pharmacol.* **1997**, *53*, 121.
- Liu, Z.-Z.; Wang, Y.; Tang, Y.-F.; Chen, S.-Z.; Chen, X.-G.; Li, H.-Y. *Bioorg. Med. Chem. Lett.* **2006**, *16*, 1282.
- Altmann, K. H. *Curr. Pharm. Des.* **2005**, *11*, 1595.
- Pinacho Crisóstomo, F. R.; Padrón, J. M.; Martín, T.; Villar, J.; Martín, V. S. *Eur. J. Org. Chem.* **2006**, 1910.
- Córdova, I.; León, L. G.; León, F.; San Andrés, L.; Luis, J. G.; Padrón, J. M. *Eur. J. Med. Chem.* **2006**, *41*, 1327.
- Pungitore, C. R.; León, L. G.; García, C.; Martín, V. S.; Tonn, C. E.; Padrón, J. M. *Bioorg. Med. Chem. Lett.* **2007**, *11*, 1332.
- (a) Pungitore, C. R.; Ayub, M. J.; Borkowski, E. J.; Tonn, C. E.; Ciuffo, G. M. *Cell. Mol. Biol.* **2004**, *50*, 767; (b) Pungitore, C. R.; Ayub, M. J.; García, M.; Borkowski, E. J.; Sosa, M. E.; Ciuffo, G.; Giordano, O. S.; Tonn, C. E. *J. Nat. Prod.* **2004**, *67*, 357.
- Pratt, W. B.; Ruddon, R. W.; Ensminger, W. D. In *The Anticancer Drugs*; Oxford University Press: Oxford, UK, 1994.
- Mangion, I. K.; MacMillan, D. W. C. *J. Am. Chem. Soc.* **2005**, *127*, 3696.
- (a) Brown, S. P.; Brochu, M. P.; Sinz, C. J.; MacMillan, D. W. C. *J. Am. Chem. Soc.* **2003**, *125*, 10808; (b) Zhong, G. *Angew. Chem., Int. Ed.* **2003**, *42*, 4247; (c) Hayashi, Y.; Yamaguchi, J.; Hibino, K.; Shoji, M. *Tetrahedron Lett.* **2003**, *44*, 8293.
- Allinger, N. L. *J. Am. Chem. Soc.* **1977**, *99*, 8127.
- Mohamadi, F.; Richards, N. G. J.; Guida, W. C.; Liskamp, R.; Lipton, M.; Caufield, C.; Chang, G.; Hendrickson, T.; Still, W. C. *J. Comput. Chem.* **1990**, *11*, 440.
- Still, W. C.; Tempczyk, A.; Hawley, R. C.; Hendrickson, T. *J. Am. Chem. Soc.* **1990**, *112*, 6127.
- Haasnoot, C. A. G.; De Leeuw, F. A. A. M.; Altona, C. *Tetrahedron* **1980**, *36*, 2783.

15. Miranda, P. O.; Padrón, J. M.; Padrón, J. I.; Villar, J.; Martín, V. S. *ChemMedChem* **2006**, *1*, 323.
16. Monks, A.; Scudiero, D. A.; Skehan, P.; Shoemaker, R. H.; Paull, K. D.; Vistica, D. T.; Hose, C.; Langley, J.; Cronice, P.; Vaigro-Wolf, M.; Gray-Goodrich, M.; Campbell, H.; Mayo, M. R. *J. Natl. Cancer Inst.* **1991**, *83*, 757.
17. Mizushima, Y.; Xu, X.; Murakami, C.; Okano, T.; Takemura, M.; Yoshida, H.; Sakaguchi, K. *J. Pharmacol. Sci.* **2003**, *92*, 283.
18. Alao, J. P. *Mol. Cancer* **2007**, *6*, 24.
19. Armarego, W. L. F.; Perrin, D. D. In *Purification of Laboratory Chemicals*, fourth ed.; Butterworth-Heinemann: Oxford, 1996.